Semi-insulating InP solid state detector and solar $pp/^7$Be neutrino experiment

Y. Fukuda [a] T. Izawa [c] Y. Koshio [b] S. Moriyama [b] T. Namba [b]
T. Sato [a] M. Shiozawa [b] and Y. Takeuchi [b]

[a] *Faculty of Education, Miyagi University of Education, 149, Aobaku-aza-aoba, Sendai, Miyagi 980-0845, Japan*

[b] *Kamioka Observatory, Institute for Cosmic Ray Research, University of Tokyo Higashi-Mozumi, Kamioka-cho, Hida, Gifu 506-1205, Japan*

[c] *Solid State Devision, Hamamatsu Photonics K.K. 1126-1, Ichino-cho, Hamamatsu, Shizuoka 435-8558, Japan*

Abstract

New radiation detector using semi-insulating indium phosphide (InP) crystal has been developed in recent years, and some bulk size detectors with a large volume (7 mm $\times$ 7mm $\times$ 0.5mm) was tested in a room temperature. We will report the present status of the development and discuss about the possibility of detection for solar $pp/^7$Be neutrinos in near future.

Key words: , solar neutrinos, neutrino oscillation, *pp* neutrinos

1 Introduction

In 1998, Super-Kamiokande has established a dramatic evidence that the muon neutrinos oscillate into tau neutrinos in the atmospheric neutrino data(1). K2K experiment is running to confirm this evidence using artificial muon neutrino beam produced by 1 GeV Proton Synchrotron at KEK (Tsukuba) with respect to Super-Kamiokande. On the other hands, Super-Kamiokande has observed solar neutrinos produced by ^{8}B beta decay, and measured both flux and energy spectrum (2). The results predicted strongly electron neutrino oscillation. In 2001, SNO (Sudbery Neutrino Observatory) experiment reported their first result using D_2O charged current reaction(3), and both SK and SNO results established ν_e oscillation and the ^{8}B solar neutrino flux was consistent with the prediction from the standard solar model(4). Moreover,

all solar neutrino experiment suggest us an unique oscillation solution on the LMA region. Recently, KamLAND experiment published their first result(5), and the result agree with the LMA and make a restriction on the LMA region.

Next step of the investigation for neutrino physics should be to measure the precise oscillation parameter and CP phase. For the future solar neutrino experiment, in particular, the oscillation mixing angle θ_{12} should be measured in detail, and should be get a flux from $pp/^7$Be reaction directly to confirm both solar and astronomical physics issue. The dominant part of solar neutrinos are released by initial processes in $proton - proton$ cycle. Most important issue for next generation solar neutrino experiments is to measure both pp and ^{7}Be neutrino flux precisely in real-time. These neutrinos have so low energy ($\leq$ 1MeV) that there might be many difficulties due to not only technique but also a backgrounds. Many possible plans are proposed by CLEAN(6), HERON(7), and XMASS(8) with noble gases as a target. KamLAND and BOREXINO are using a liquid scintillator to detect ^{7}Be solar neutrinos.

2 Indium detector for solar neutrino experiment

In 1976, Raghavan proposed new technology to detect electron neutrinos, especially low energy $pp/^7$Be solar neutrinos(11) using ^{115}In. Many possible detectors using indium were designed in last two decade, however no realistic detector was established yet. An ^{115}In has a cross section to capture electron neutrinos (ν_e) via following reaction;

$$^{115}\mathrm{In} + \nu_e \rightarrow {}^{115}\mathrm{Sn}^* + e^-, \quad (1)$$

$$^{115}\mathrm{Sn}^* \rightarrow {}^{115}\mathrm{Sn} + \gamma_1(116keV) + \gamma_2(497keV). \quad (2)$$

The Q-value of above reaction is 128 keV, so the prompt electron could be used for the neutrino spectroscopy. An excited state of ^{115}Sn decays into the ground state with 4.76 μs lifetime, and emits two gammas. Therefore these are used as triple-coincident technique in order to distinguish huge backgrounds and signal. However, ^{115}In itself has a beta decay into the ground state of ^{115}Sn with a lifetime 4.6×10^{12} year. Therefore, fine segmented and high energy resolution detector should be needed. A detector based on metal loaded liquid scintillator was proposed by LENS(12). Other possibility to use InP pn-junction semiconductor was developed in 1987 (13). This paper will report another possibility using semi-insulating InP semiconductor for radiation detector.

The semi-insulating (SI) InP wafer is produced by several methods. Typical material is doped by Fe and the crystal is grown by the liquid encapsulated Czochralski (LEC) method. However, the lack of a rectified contact on SI InP

produces high leakage current in these devices. The ESTEC group have characterized a 0.18 mm thick of InP at -60 °C achieving 8.5 keV FWHM at 60 keV(9), and Pelfer's group obtained 11 keV FWHM at 122 keV with 0.25 mm thick SI InP at -60 °C(10). There is other crystal growth method namely called the Vertical Gradient Freeze technique (VGF), which is relatively higher resistance it naturally has relatively higher resistance and smaller EPD than LEC material. This indicates that it might be possible to produce a bulk size detector, and it should be used for solar $pp/^{7}$Be neutrino detector. The schematic view of the SI InP detector for solar $pp/^{7}$Be neutrinos is shown in Fig.1. According to Raghavan's calculation, about $1pp\nu_e$ per day is predicted by modest 4ton mass of ^{115}In(15). Assuming the bulk size of SI InP detector with size of 8 cm $\times$ 8 cm $\times$ 0.5mm, the detector weight is 15 g ($\rho = 4.79$ gcm^{-3}), which corresponds to 12 g of indium. The natural abundance of ^{115}In is about 96%, so it needs about 340,000 detectors for 4 tons mass of ^{115}In. This is quite larger number of channels than Super-K, but it should not be surprised because of typical X-ray astronomical telescope has a order of 100,000 channels of the detector. The detector simulation of the solar pp neutrinos measurement as-

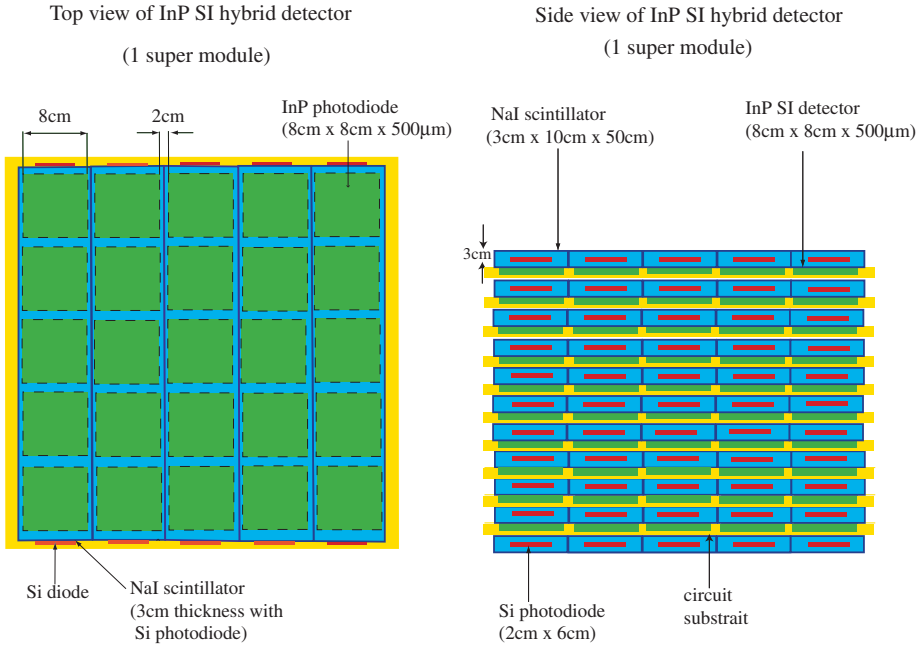

Fig. 1. Schematic view of hybrid InP detector for $pp/^{7}$Be neutrinos measurement.

suming the configuration shown in Fig.1 used as 1 super-module is done by GEANT simulator. It is also assumed to have the energy resolution of 10 % at 100 keV. This is almost same performance as above groups, but we would expect much larger size of detector. Figure 2 shows the energy spectrum of the prompt electron which is observed at centered SI InP detector, and the energy spectrum of γs observed by both centered InP and the surrounded NaI scintillator. Centered InP detector is assumed to observe the prompt electron, and photo-electron from γ_1 and the Compton electron from γ_2, and the sur-

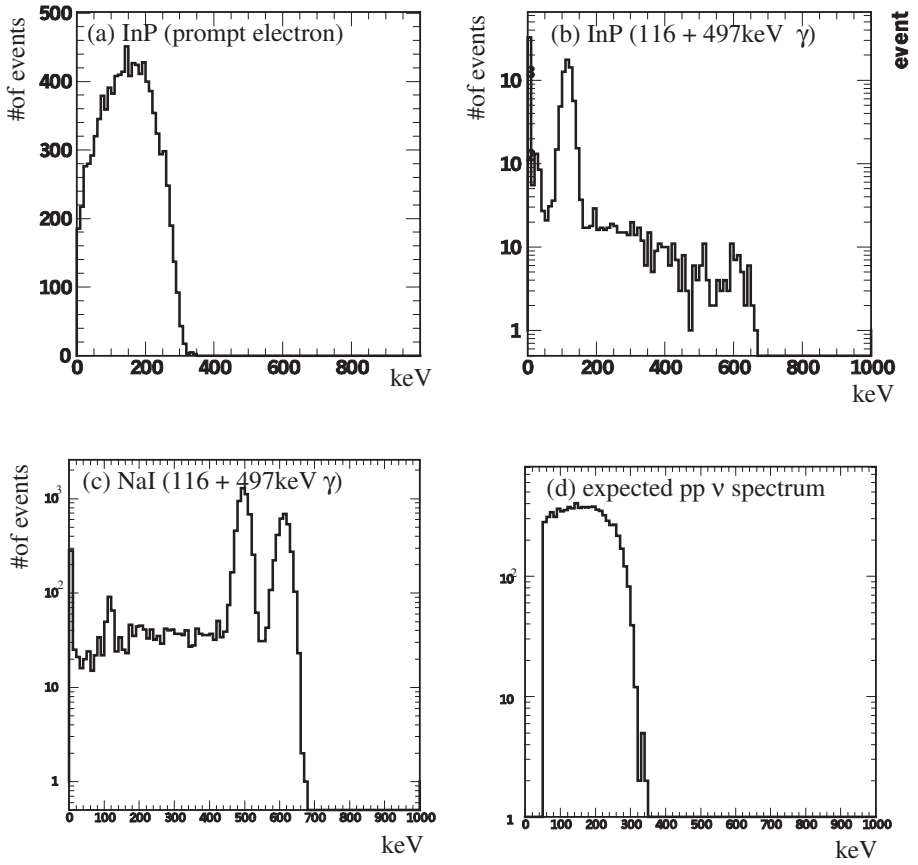

Fig. 2. Simulation of *pp* neutrinos measurement by the hybrid InP detector. Assuming InP detector has an energy resolution 10 % at 100 keV, and the neutrino capture occurs at the centered InP detector of the super module. Each figures show the energy spectrum of (a) prompt electron in target InP, (b) γ_1 and γ_2 in same InP, (c) γ_1 and γ_2 in surrounded NaI, and (d) the expected *pp* neutrinos, respectively. The detection efficiency is estimated by about 80 %.

rounded NaI scintillator observes partial photo-electron from γ_1 and residual fraction of Compton scattering from γ_2. Trigger condition is briefly 2-fold of the prompt electron and γ_1 within same InP detector, or surrounded NaI scintillator within a proper time, and the other NaI should have energy deposit and their summing energy should be large than 300 keV. Using this scheme, the detection efficiency of *pp* neutrinos by 1-super module is estimated by 80 %.

3 InP proto-type detector

The wafer of VGF SI InP is delivered by the AXT Co.Ltd. The natural radioactive background such as U/Th series including the material is very important because the unknown background makes us difficult to detect rare solar neu-

trino events. In fact, the ultra low background germanium detector located in the Kamioka mine was used for the measurement of X-ray/γ-ray emitted from the SI InP wafer itself. Fig.3 shows the energy spectrum of those γs caused by U/Th fission processes. The amount of SI InP wafer is 15 g which corresponds to 12 g of ^{115}In. From the yield calculation using known peak, the amount of

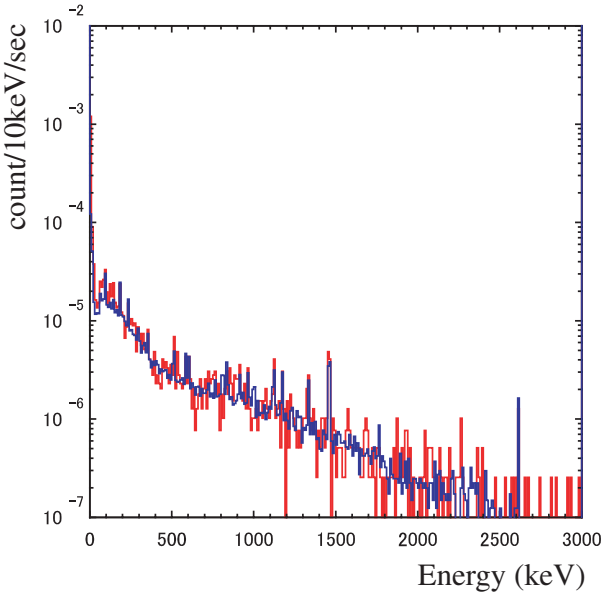

Fig. 3. The γ energy spectra emitted from U/Th series included by SI InP wafer by the ultra low background Germanium detector. Blue and red lines correspond to the spectra with/without InP wafer, respectively.

U/Th series in SI InP wafer is estimated by less than 5×10^{-11} and 3×10^{-11} g/g, respectively. This indicates that the material itself is very clean material, and the background initiated by un-removable radio-active source is negligible. Using this wafer, the proto-type SI InP detector was produced by Solid State Division on Hamamatsu Photonics K.K. The schematic view and actual surface photo-graph of the present proto-type detector is shown in Fig.4. The detector size is 7 mm $\times$ 7 mm $\times$ 500μm and the electrodes consist of Cr-Au with 1 μm in thickness for top and Au-Ge/Ni/Au with 0.13/0.015/0.5 μm in thickness for bottom. The junction of those electrodes with InP is made by the ohmic contact. The leakage current as a function of the bias voltage is shown in Fig.5. Here, the current was measured by the positive bias for top electrode. Typical current is 40 μA at 500 V in a room temperature. The current is not changed either positive and negative bias applied.

4 Response of InP proto-type detector

The performance of SI InP detector was measured by using radio active sources. The setup logic is shown in Fig.6. We used ^{241}Am for α-particle source

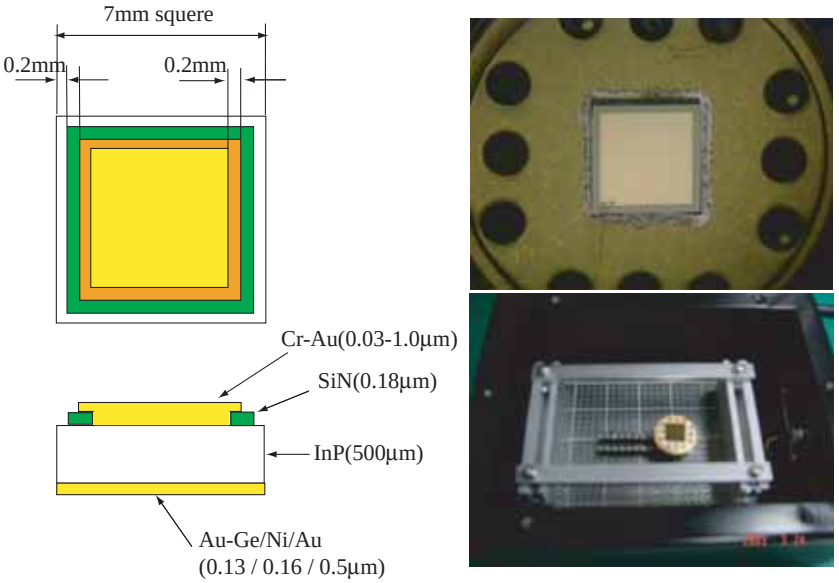

Fig. 4. Left figure shows the schematic view of the proto-type detector. The detector size is 7 mm $\times$ 7 mm $\times$ 0.5 mm. The area of top electrode is 6 mm $\times$ 6 mm. Right photo-graphs show expanded top view of the detector and the entire view mounted on the test bench.

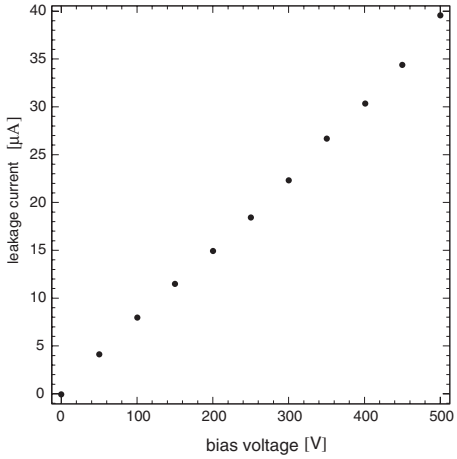

Fig. 5. The leakage current as a function of bias voltage. Basically the current is not changed even though the positive or negative bias voltage.

and ^{57}Co, ^{133}Ba, ^{137}Cs and ^{60}Co for γ-ray source, respectively. Fig.7 shows observed charge distribution of the α particle at 3 kV bias voltage. Here, in order to avoid the saturation of the gain in the charge amplifier, the energy of α particle should be reduced by almost 1.8 MeV due to the energy loss in the air between the detector and the radio-active source. As shown in the Fig.7, the single peak could not be observed even though the energy resolution was assumed by 4 % which is assumed by the observation of γ-rays as shown in later, however, the peak is not seen in the observation by Si diode too. This is the absorption effect by the air. The expected energy deposit of α-particle in

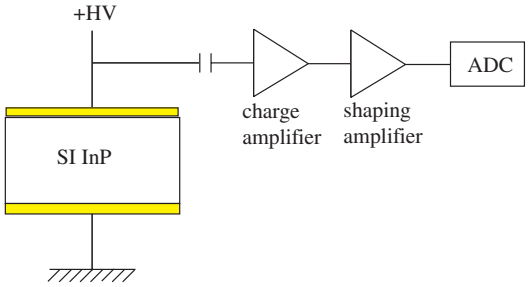

Fig. 6. Configuration of radiation measurements with SI InP proto-type detector. The high voltage is applied by positive at the top electrode.

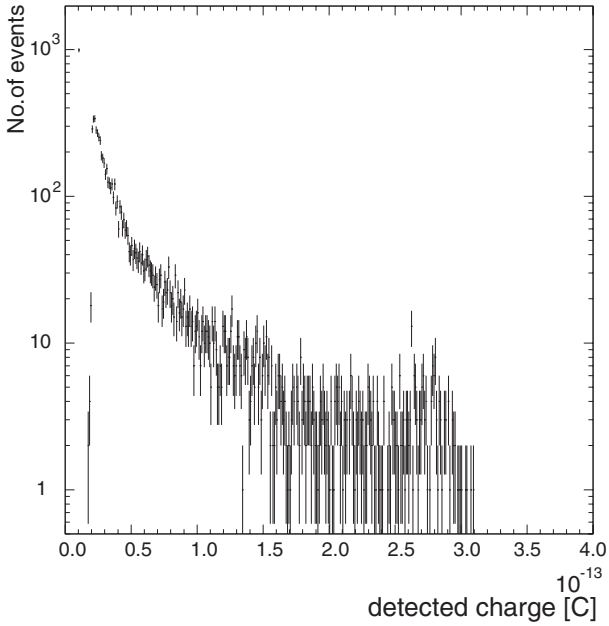

Fig. 7. Observed charge distribution of α-particle at 3kV bias voltage. Here, the energy of α-particle is calibrated by 1.8 MeV in order to avoid the signal saturation.

the InP is 1.8 MeV due to the energy loss in air and some materials, and the energy calibrated by Si diode. The obtained spectrum continues up to 3×10^{-13} C, therefore the energy of carrier production is obtained by 0.9 eV. This is not same as the energy estimated by γs and the penetrating muons described later. However, both energies itself are quite smaller than the referenced value of 4.2 eV.

Generally speaking, an average energy to create electron-hole pair of Si is 3.6 eV at room temperature. According to some references, an averaged energy of the electron-hole pair production for InP is 4.2 eV at room temperature. It is relatively higher value than the value of Si diode. However, the observed charge from α-particle is much larger than the expected value. The obtained charge indicated the energy to be order of 0.9 eV instead of 4.2 eV, if the charge collection efficiency (CCE) is assumed to 100 %, or if the diffusion

length ($L_d \equiv \mu\tau\frac{V_0}{d}$, here μ is carrier mobility, τ is life-time of the carrier trapping, V_0 is the bias voltage, and d is thickness of the detector) is assumed to be a few hundred μm, which is much longer then the range of α particle in InP. The estimated energy is almost quarter of the referenced value, and the results is quite impressive.

We estimated that this is the energy to create electrons by the ionization, not an electron-hole pair production, and the above α-particle spectrum are obtained by the *solid state chamber* instead of *semiconductor*. The energy of electron-hole pair production (4.2 eV) is naturally consistent with the band gap of InP *semiconductor* (1.29 eV) compared with the case of Si. On the other hands, the ionization of electrons is usually an order of 0.1 eV in the case of gas chamber. That is the reason why we regards as the *solid state chamber* for the proto-type detector. The range of α-particle in the InP is almost less 10μm, and this short range is not useful for estimating of the diffusion length. In order to evaluate the diffusion length and the ionization energy simultaneously, the charge distribution of γ-ray should be used.

5 Response for γ-rays

Figure.8 shows that the observed spectra of ^{133}Ba, ^{137}Cs, and ^{57}Co. It is clearly seen the photo-electric peak of 356 keV γs from ^{133}Ba, but only the bump was appeared for 122 keV photo-peak from ^{57}Co , and no peak for 662 keV γ from ^{137}Cs was found. The common feature is same kinds of tail, which is seen in the charge spectrum of α particle shown in Fig.7, are also seen in Fig.8. As discussed in the previous section, present proto-type detector might have non-uniform quality of the diffusion length of carrier. The range of photo-electron for each γs are almost 100, 200 and 945 μm, respectively. Therefore the diffusion length should be larger than 200 μm, but might be same order of a few hundred μm in a good quality region. However, for bad quality region, it might be less than the order of 10 μm. However, the observed charge depends on both the diffusion length and the carrier production energy as shown in Eq.4. In order to estimate both the diffusion length and the carrier production energy simultaneously, the simulation was done by those as free parameters. The generated charge was calculated by the following formula;

$$Q_{total}[C] = \frac{E_e}{\epsilon} \times e. \tag{3}$$

Here, E_e is the energy of electrons which is generated by photo electric effect or the Compton scattering, ϵ is ionization energy, and e is the electric charge (1.602×10^{-19} C). The observed charge was simulated by considering the

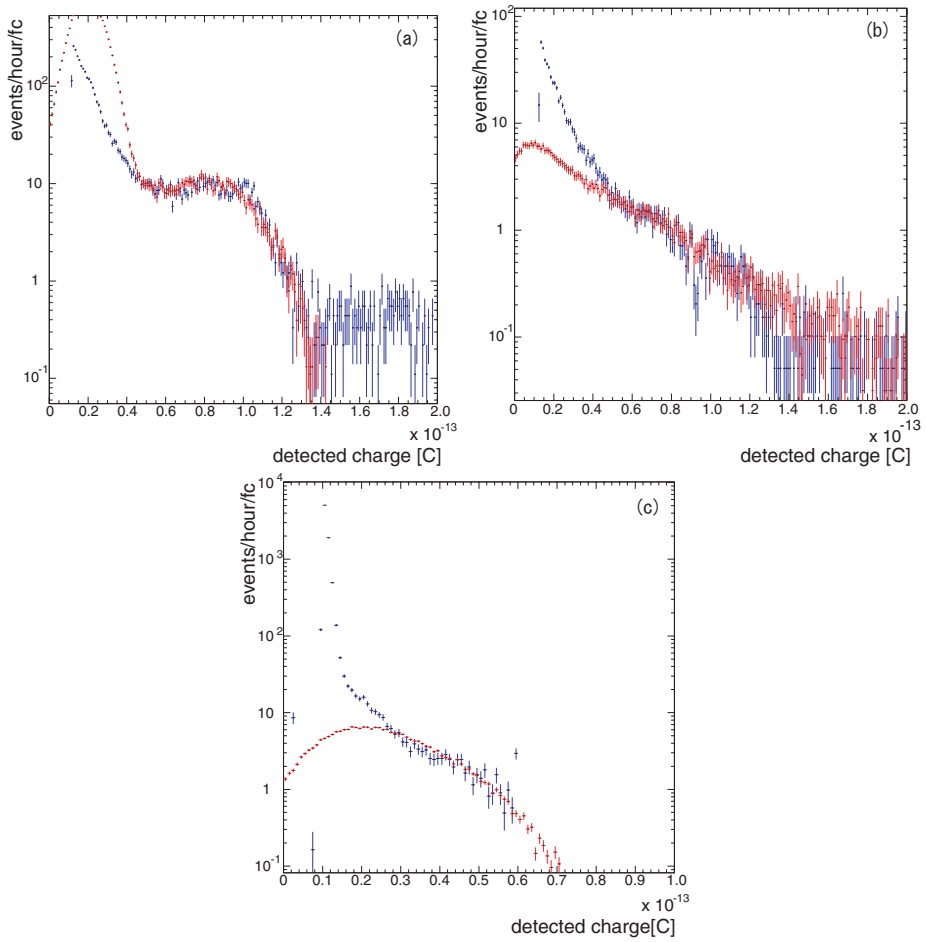

Fig. 8. Observed γ-rays from (a) ^{133}Ba, (b) ^{137}Cs and (c) ^{57}Co radio-active source, respectively. The background has already been subtracted by using blank run data. The 356 keV photo-peak is clearly found in figure (a), but no peak from 662 keV and 122keV γs in figure (b) and (c). Blue and red points correspond to the data and simulation with best fit parameters which will be obtained by data analysis, respectively.

diffusion length as follows;

$$Q_{obs}[C] = \int_0^R \frac{dE}{dx} \times \frac{1}{\epsilon} \times e^{-\frac{r(x)}{L_d}} dx. \tag{4}$$

Here, R is electron's range, $r(x)$ is the distance between the positive electrode and the position on the electron range with a fraction of dx, L_d is the carrier diffusion length, $\frac{dE}{dx}$ is the energy deposit in a fraction of dx, and ϵ is an ionization energy. If the diffusion length have large enough to the thickness of detector, the CCE could achieves almost 100 %.

In the simulation, the diffusion length is assumed to be 50 to 2000 μm in a 50 μm step, and the ionization energy is assumed by 0.2 to 1.2 eV in a 0.1 eV step. Figure.9, 10 and 11 show the χ^2 distribution as a function of both diffusion length and the ionization energy for ^{133}Ba, ^{137}Cs, and ^{57}Co, respectively. The minimum χ^2 was commonly obtained by 0.3 - 0.4 eV for the ionization energy and 300 - 500 μm for the diffusion length in each distribution. Using best fit parameters for each distribution, the charge distribution obtained by simulation are also shown in Fig.8. The obtained best fit values of the ion-

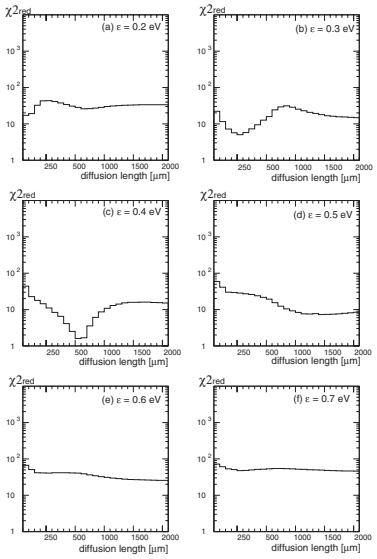

Fig. 9. χ^2 plots for each diffusion length and the ionization energy for spectrum of ^{133}Ba. The best fit parameters are obtained by $\epsilon = 0.4$ eV and $L_d = 500\mu$m.

ization energy 0.4 eV is not consistent with the result from α-particle, and almost half of the value. It might be possible to explain the reason why those numbers are different that the *Quenting factor*. However, the carrier produced by the ionization by electron is much realistic for the solar $pp/^7$Be neutrino observation.

Another calibration could be done by the penetrating muons though the proto-type InP detector. At the ground level, the muon has about unique momentum 1 GeV/c, and makes a energy deposit with a minimum ionization. From the calculation, the energy deposit is estimated by about 350 keV in the 500 μm SI InP wafer. Figure.12 shows the charge distribution of the penetrating muons. According to the simulation assuming by 0.40 eV for the ionization energy and 300/500 μm for the diffusion length, the expected charge is obtained by 6.6/8.6 $\times 10^{-14}$ C. It is very consistent with data and simulation. Therefore, the ionization energy 0.4 eV and the diffusion length 300 - 500 μm are very crude values of our proto-type detector.

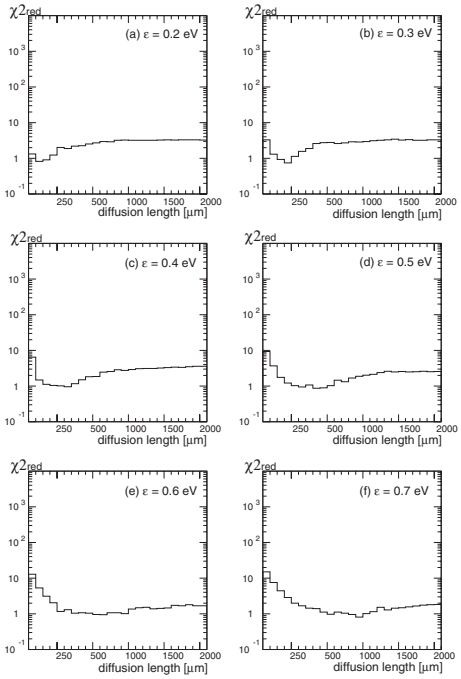

Fig. 10. χ^2 plots for each diffusion length and the ionization energy for the spectrum of ^{137}Cs. The best fit parameters are obtained by $\epsilon = 0.3$ eV and $L_d = 200\mu$m.

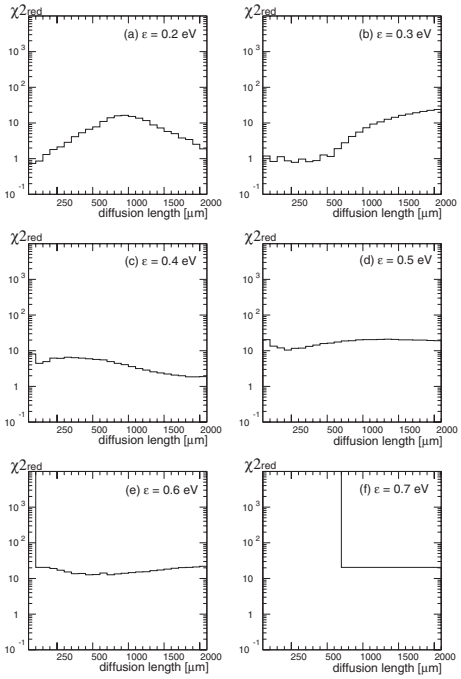

Fig. 11. χ^2 plots for each diffusion length and the ionization energy for the spectrum of ^{57}Co. The best fit parameters are obtained by $\epsilon = 0.3$ eV and $L_d = 350\mu$m.

7 Future prospect

In term of the realization for the solar neutrino detector, we need to establish the method to produce good quality in the larger area such as 64 cm^2. In

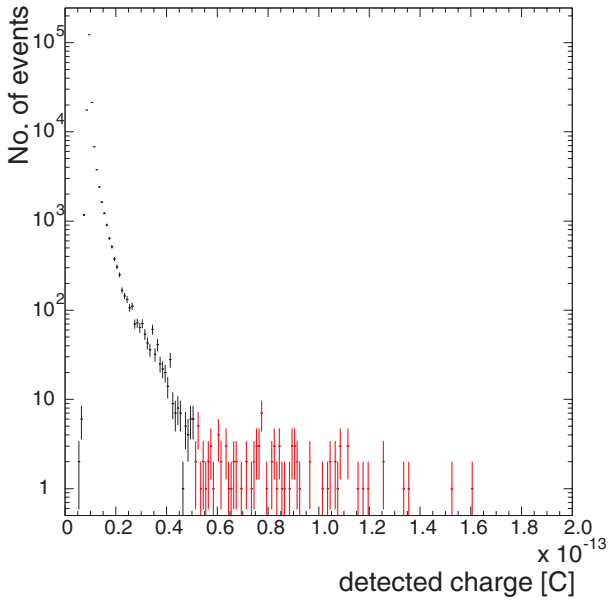

Fig. 12. Observed charge distribution of penetrating muons as shown in red data points. The simulations assumed by the $\epsilon = 0.4$ eV and $L_d = 300 - 500\mu$m are consistent with the data. The huge backgrounds observed below 400 fC caused by the leakage current.

such case, we also need to demonstrate the detector performance at lower temperature around -60 °C, because of the reduction of leakage current. In a low temperature environment, the leakage current becomes quite smaller according to the following formula;

$$I[A] \propto T^{\frac{2}{3}} exp(\frac{-E_g}{2k_B T}) \tag{5}$$

where T is the temperature, E_g is band gap, and k_B is the Boltzmann constant. In fact, we measured the leakage current was 0.018 μA at 100 V bias voltage in case of -40 °C. This is almost order of 1/100 compared to the room temperature. Lower leakage current gives us not only lower noise level, which is directly related to the detector performance if the detector area becomes large, but also longer diffusion length of the electron (16). Therefore we could expect the improvement of CCE at low temperature. In order to demonstrate these effects, we have already prepared new proto-type detector, which have same structure as present proto-type but mounted on the Peltier cooler as shown in Fig.13. We will soon check the detector performance of this detector. Another proto-type detectors, which is also same structure but half thickness, have been prepared already in order to confirm the present detector performance such as the diffusion length and the electron production energy.

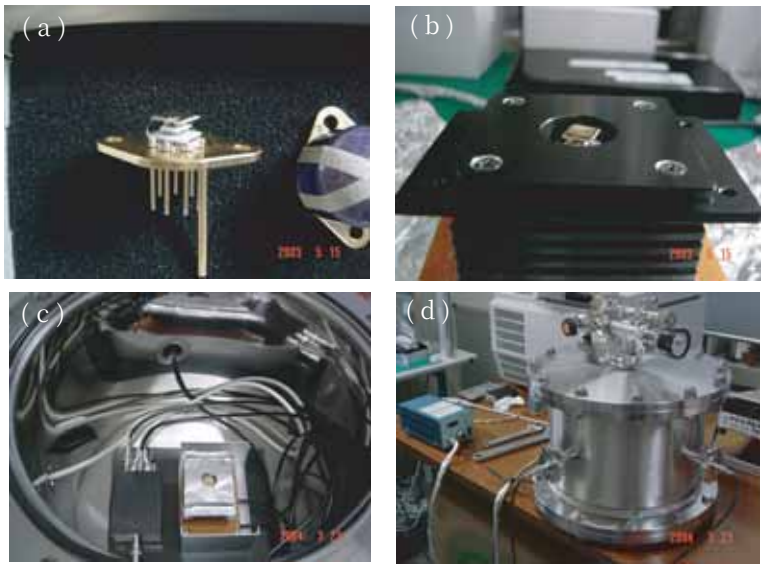

Fig. 13. (a)New proto-type detector mounted on the Peltier cooler, (b) mounted on the radiator, (c) located in the vacuum chamber, and (d) whole setup of the cooling system with vacuum pump.

8 Conclusion

The proto-type detector with the SI InP has been developed, and tested by using several radiation sources for measurement of performance. Observed charge distributions show that the proto-type detector has 0.4eV for the electron production due to the ionization, and the proto-type detector collects those charge like as a *solid state chamber*. The charge collection efficiency is almost 80 % for the case of α-particle, but 50 % for the case of γ-ray. This is well explained by the diffusion length to be order of 300 - 500 μm. This is the first time to demonstrate the SI InP detector with a bulk size crystal, and the detector performance shows us that it is possible to use bulk size SI InP for the solar $pp/^{7}$Be detector, if we could establish the way to control the quality for the electrode contact.

Acknowledgments

This work was supported by the Grant-in-Aid Scientific Research (B)(2) 13440066 of Japanese Society for the Promotion of Science.

References

[1] Y.Fukuda *et.al,* Phys. Rev. Lett. **81** (1998) 1562.

[2] S.Fukuda *et.al,* Phys.Rev.Lett. **86** (2001) 5651.
[3] SNO Collaboration Phys.Rev.Lett. **87** (2001) 071301.
[4] J.N.Bahcall, M.H.Pinsonneault, S.Basu, Astrophys.J. **555** (2001) 990.
[5] KamLAND collaboration, Phys.Rev.Lett. **90** (2003) 021802.
[6] D.N.McKinsey and J.M.Doyle, J.of Low Temp. Phys. **118** (2000) 153.
[7] R.E.Lanou, H.J.Maris, and G.M.Seidel, Phys. Rev. Lett. **58** (1987) 2498.
[8] Y.Suzuki hep-ph/0008296
[9] A.Owens *et. al,* Nucl. Instr. and Meth. A487 (2002) 435.
[10] P.G.Pelfer *et. al,* Nucl. Instr. and Meth. A458 (2001) 400.
[11] R.S.Raghavan Phys. Rev. Lett. **37** (1976) 259.
[12] R.S.Raghavan Phys. Rev. Lett. **78** (1997) 3618.
[13] Y.Suzuki, Y.Fukuda, Y.Nagashima, and H.Kan Nucl. Instr. and Meth. **257** (1989) 142.
[14] H. El-Abbassi, S. Rath and P. J. Sellin Nucl. Instr. and Meth. **466** (2001) 47.
[15] R.S.Raghavan hep-ex/0106054.
[16] J.Costa and A.Peczalski J.Appl.Phys. **66** (1998) 674.